

An Improved Tracking Technique for Assessment of High Resolution Dynamic Radiography Kinematics

G. Papaioannou¹, C. Mitrogiannis¹ and G. Nianios¹

Summary

Previous attempts to track skeletal kinematics from sequences of images acquired using biplane dynamic radiography report challenges in automating the tracking technique due to image resolution issues, occlusion from segments appearing synchronously in the field of view and computational load. This translates into many hours of manual work to export the kinematics. The proposed new tracking method tackles the above problems and reduces the time to export kinematics from several hours to less than 3 minutes.

Introduction

Dynamic assessment of three-dimensional (3D) skeletal kinematics is essential for understanding normal joint function as well as the effects of injury or disease. Current non-invasive or minimally invasive methods for evaluating in-vivo knee arthrokinematics are inadequate for accurate determination of dynamic joint function due to limited accuracy and/or insufficient sampling rates[1-3]. A 3D marker-based tracking (MBT) method is presented to estimate in-vivo skeletal motion of the knee from high-speed sequences of biplane radiographs. The method implicitly assumes that geometrical features cannot be detected reliably and an exact segmentation of bone edges is not always feasible. An existing biplane radiograph system was simulated as two separate single-plane radiograph systems and static and dynamic errors were estimated.

Methods

Two subjects (Males: 38 and 42 yrs) with ACL reconstructed knee and healthy contra-lateral knee were selected from an ongoing study of ACL reconstruction (approved by our institutional IRB). After obtaining informed consent, 1.6mm tantalum markers were implanted in the distal femurs and proximal tibia of each joint (3 per bone) at the time of ACL reconstruction surgery. In-vivo 3D knee kinematics was acquired 3 years after ACL reconstruction during one-legged forward hopping (sub-maximal, hop distance 50% of lower limb length) using a new high-speed (both at 250 and 480frames/s) and high-resolution (with both 512x512 and 1024x1024 pixel) dynamic radiography instrumentation (DRSA) (fig. 1). The new instrument's greater resolution along with larger field of view improved significantly the projections of the knee joint and minimized occlusions [3, 4]. The new algorithm employs image-processing routines (Laplacian filter, Canny edge detec-

¹Human Movement Sciences, Bioimaging and Advanced Biomechanics laboratory, University of Wisconsin Milwaukee, Milwaukee, WI, USA

tion and homegrown routines) to the marker's geometry properties (shape and diameter). A projection of a 1.6mm tantalum marker on 2D plane with 512x512 resolution created a region of 20 to 30 pixels. The 1024x1024 images produced always at least a doubling in the number of pixels available for tracking (fig. 1).

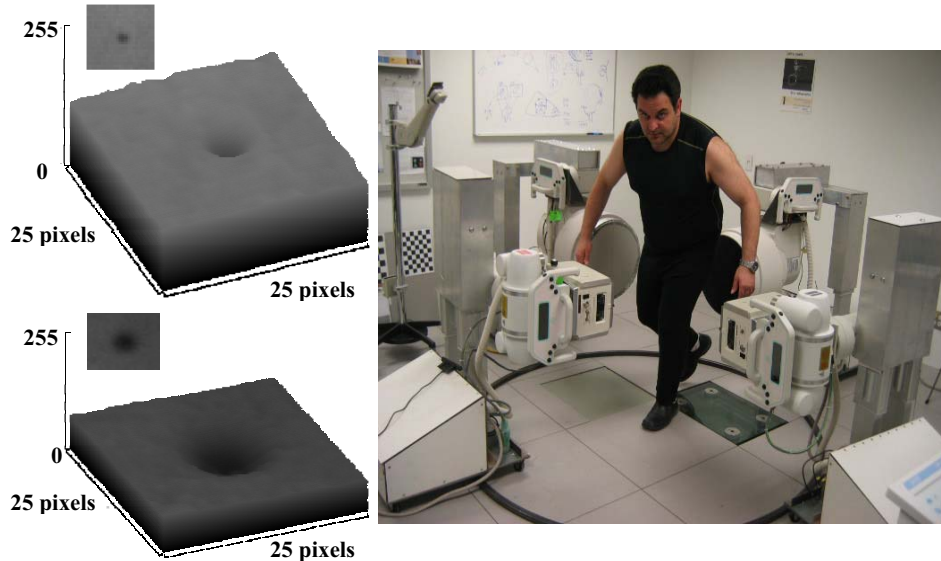


Figure 1: Tantalum Marker Surface Plot Diagram for 512x512, (top left) and 1024x1024 pixels (below right) and subject performing single leg hopping task at the DRSA instrument (right).

At high resolution, increasing the data acquisition rate reduces the displacement of the marker in the x, y-coordinates from frame to frame to less than 13 pixels. A 5x5 Laplacian filter was applied on a small area around the marker's region in order to enhance the contrast (fig.2) and remove the useless information (background) close to the marker.

Performance of the Biplane Radiographic system was assessed using a test object consisting of four 5x5x1.25cm plates of acrylic plastic. Three 1.6mm tantalum spheres were placed flush with the top surface of one of the plates in a right isosceles triangle with 3cm legs. The 4 plates were then cemented together to create a 5cm cube with the marker triangle in the center. Static precision (a function of system noise) was assessed with the test object positioned stationary in the center of the field of view. Dynamic errors were assessed by suspending the object from a stiff elastic band and then dropping it (increased rotational motion), allowing it to twist and bounce throughout the field of view. For each test, 125-1000 images were acquired at 250 frames/s with an exposure (shutter) time of 500 μ s. X-ray system protocols were 60 kVp, 60mA, 0.5 s with low (512x512) and high resolution

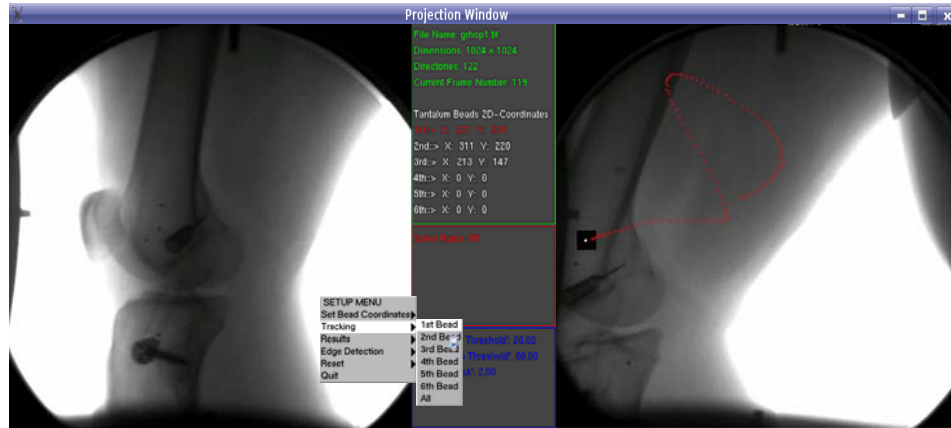


Figure 2: Snapshot during the marker tracking (left) and synchronous displacement history of the selected marker projected in real time on a plot diagram (right).

(1024×1024) trials. This was thought to be a reasonable simulation of the types of measurements made of tibiofemoral motion, since the markers in the phantom are identical to those used in human studies and their spacing and distribution are similar. In the human studies 3D coordinates of implanted markers were determined for 10 single legged hopping trials from DRSA with dynamic accuracy of $\pm 0.1\text{mm}^{[1]}$.

Results and Discussion

During the dynamic tests, the cube moved through a 550cm^3 volume. Typical image signatures for the 1.6 mm markers were approximately 4x4 pixels, which was consistent with the estimated pixel size for the low-resolution experiment ($250\text{mm FOV}/512 \text{ pixels} = \sim 0.5\text{mm/pixel}$, plus non-perfect focus of X-ray source and optics). These values for the high-resolution experiment were at least 10x10 pixels ($400\text{mm FOV}/1024 \text{ pixels} = \sim 0.39\text{mm/pixel}$). The 3D vector distances (in mm) between the pairs of markers for the low and high-resolution experiments for every frame in the movement sequence suggested that: Measured distance (mean) in the static experiment was 29.90 mm and the dynamic accuracy (raw data) was also 29.90mm. Typical Error (SD from mean) was ± 0.02 and ± 0.10 respectively. The worst-Case Error (max minus min error) was ± 0.07 and ± 0.18 respectively. Static and raw dynamic results are based on raw (unfiltered, unsmoothed) 3D coordinates. Error magnitude was consistent throughout the field of view. The means were consistent between the static and dynamic data sets. Upon observing the raw error plots (Figure 3a), it appeared that there were both low and high frequency components. Dynamic errors averaged $\pm 0.1 \text{ mm}$ (1/5th of the pixel size), demonstrating the benefits of gray-scale centroids for finding marker centers with sub-pixel accuracy. 3D calibration and distortion correction were not significant factors, based on the uniformity of the errors across the field of view.

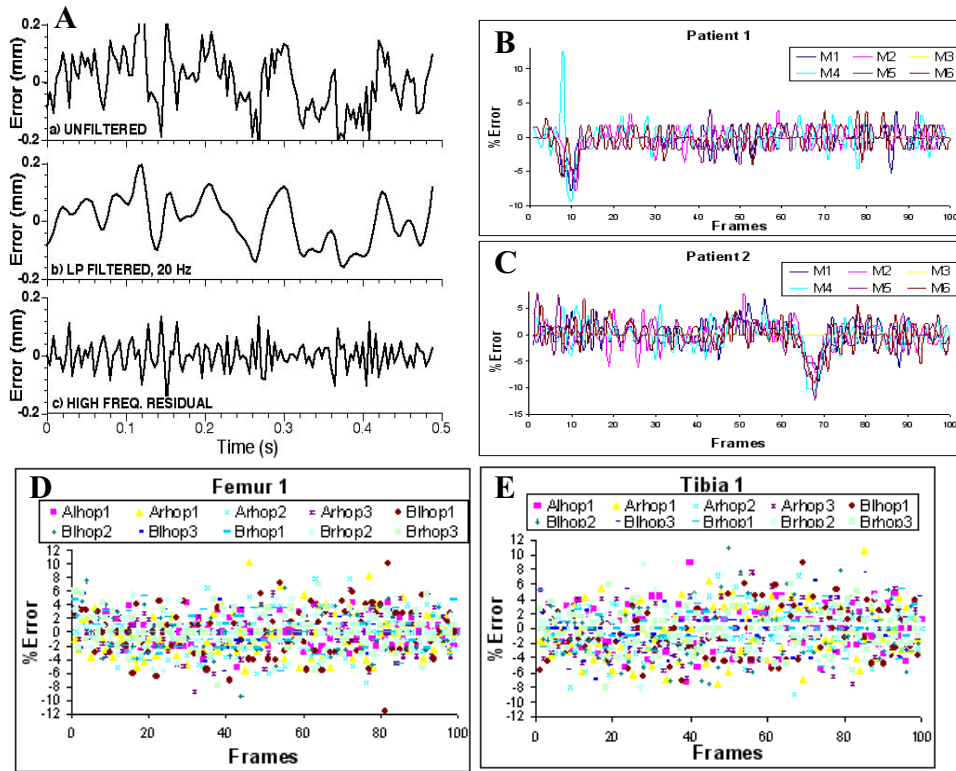


Figure 3: A) 3D Errors, dynamic cube study, calculated as the inter-marker distance for each frame minus the mean distance. a) raw (total) errors. b) Errors after optimal smoothing. c) Residual, high-frequency errors (a minus b), B) In human trials dynamic error was expressed as gray level percentage difference of each marker's centroid gray level from frame to frame: here % Error for femoral and tibial markers M1-M6 for subject one, C) same graph but for subject 2, D) percentage error for all subjects' femur markers during the hopping trials for both legs and both DRSA views E) same graph for tibia markers (glhop1 means: A and B: left and right DRSA cameras, r and l: right and left leg).

Static errors (noise-dependent) were in the order of 0.03 mm. Dynamic errors were approximately three times (two times in high resolution) as large as static errors. There are three most likely causes for this: motion blur, background effects and quantization errors due to the finite pixel size. Blur, caused by motion of the markers during the sampling interval, could shift the marker centroid positions. The 2D component of the error is a function of the relative velocity of the two markers parallel to the image plane – if they are moving at the same speed and direction in this plane, both marker centroids would be shifted by the same amount. The 3D distance between two of the test object markers was calculated for every frame in

the movement sequence. Low frequency (LF) errors were determined by optimal low pass filtering (approx. 20 Hz) the raw errors. High frequency errors are the residual left after subtracting LF errors from the raw errors. The inter-marker distance would be zero. To estimate the error contribution from blur, the Z (vertical) component of the relative velocities of the two markers was calculated. This axis had the largest velocity component, and is also parallel to both intensifier image planes (maximizing the blur effect). The average absolute difference in the Z component of velocity between the markers was 60 mm/s, causing a mean shift in the relative centroid positions of only 0.017 mm (given the 500 μ s sample period). In the human trials (n=10) dynamic error was expressed as gray level percentage difference of each marker's centroid gray level from frame to frame (figure 3). In the low-resolution trials the average error stays within 5% and in the high-resolution trials it improves to less than 3% with apparently much more gray level information around the centroid (figure 3).

The MBT software was developed and tested on three different computer systems. In all benchmarking tests the 'image Loading' time doubles when the resolution becomes quadruple while the 'Tracking' time seems to quadruplicate

Table 1: Benchmarking results for the two different image resolution experiments

Computers	Resolution	Input Image Sequence (Frames)	Loading (s)	Tracking (s)	Tracking Without Redisplay (s)
Laptop Dell	512\times512	100	1.52	6.93	1.21
		100	2.26	21.25	4.76
		485	110.24	300.26	240.12
Workstation-1	512\times512	100	1.48	5.82	0.64
		100	2.16	14.46	0.96
		485	26.96	76.20	27.78
Workstation-2	512\times512	100	0.75	0.78	0.26
		100	1.55	2.34	1.25
		485	5.82	10.64	5.45

almost in all computers (table 1). The MBT software independently of the resolution of the radiographic image sequences is capable to track fast and accurate the tantalum markers and exports the skeletal kinematics in less than three minutes without operator intervention.

This is a significant reduction in data processing particularly if the method is to be applied to the clinical environment.

References

1. Papaioannou G., Fiedler G., Nianios G., Mitroyiannis C. 2008. March 2-5. Using a direct digital radiography CCD imaging sensor in place of image intensifiers in human joint imaging. Orthopaedic Research Society, San Francisco, USA.
2. Papaioannou G., Knight R., Nianios G., Mitroyiannis C., Whitton P., Ewing J. 2007. Articular Cartilage Thickness Measurement with high resolution Computed Tomography and Magnetic Resonance Imaging: In-vivo and Cadaveric Specimen Comparisons. In *6th Combined Meeting of the Orthopaedic Research Societies*. Honolulu, Hawaii.
3. Papaioannou G., Nianios G., Mitroyiannis C. 2007. An Improved Tracking Technique for Measuring High Resolution Dynamic Radiography Skeletal Kinematics. In *6th Combined Meeting of the Orthopaedic Research Societies*. Honolulu, Hawaii.
4. You B-M, Siy P., Anderst W., Tashman S. 2001. In-vivo measurement of 3D skeletal kinematics from sequences of biplane radiographs: application to knee kinematics. *IEEE Trans. Medical Imaging*. 20: 514-25.